IOSR Journal Of Humanities And Social Science (IOSR-JHSS)
Volume 30, Issue 4, Series 3 (April, 2025) 58-64
e-ISSN: 2279-0837, p-ISSN: 2279-0845.
www.iosrjournals.org

Deformation Monitoring Of Afe Babalola Administrative Building The Federal Polytechnic Ado-Ekiti

[1]Bamidele Olabode FATEYE
Department of Surveying and Geoinformatics
The Federal polytechnic Ado-Ekiti, Ekiti State Nigeria
08069730408, fateyeolabode73@gmail.com
[2]Kehinde Hassan ISHOLA
Department of Surveying and Geoinformatics
The Federal Polytechnic Ado-Ekiti, Ekiti State Nigeria
07032373455, ishola_kh@fedpolyado.edu.ng
[3]Felix Gbenga ODEYEMI
Department of Surveying and Geoinformatics
Federal polytechnic Ede, Osun State Nigeria
08062337838, odeyemifelix939@yahoo.com

Date of Submission: 01-04-2025 Date of Acceptance: 11-04-2025

I. Introduction

Various environmental and geological factors, such as groundwater level fluctuations and tectonic activities, can induce subtle, gradual movements in engineering structures. These displacements are typically imperceptible to the human eye and occur incrementally over an extended period. The systematic investigation of structural movements is crucial for preventing potential structural failure and damage, a process known as deformation surveying.

Deformation monitoring encompasses multiple terrestrial surveying techniques, including precise leveling, theodolite measurements, total station observations, and very long baseline interferometry. The methodological approach to deformation surveys can be broadly classified into two primary categories: geodetic surveying and geotechnical structural measurements.

Geotechnical measurements specifically focus on localized deformation assessments, employing specialized instruments such as tiltmeters, strain meters, extensometers, joint meters, and laser distance gauges to capture minute structural movements with high precision.

Deformation monitoring plays a crucial role in enhancing safety, informing maintenance practices, protecting the environment, and ensuring compliance with regulatory standards. By employing advanced monitoring techniques and integrating data, professionals can make informed decisions to manage risks effectively and maintain the integrity of structures and natural features. The justification for deformation monitoring lies in its ability to provide critical information that aids in the prevention of disasters, efficient resource management, and the understanding of geological and environmental processes. In the words of Zhou *et al.,* (2019), deformation monitoring, also known as deformation survey, is the systematic measurement and tracking of alterations in the shape or dimensions of an object due to stresses induced by applied loads. The systematic measurement is essential in the monitoring of buildings, bridges, dams, and other civil engineering structures.

The study focuses on examining the deformation of the Afe Babalola Building at the Federal Polytechnic, Ado-Ekiti, particularly noting its unstable ground conditions and water-related issues during rainy seasons.

Key Literature Review Findings:
1. Monitoring Techniques and Advancements:
- Zhou et al. (2019) demonstrated GB-RAR technique's effectiveness in building deformation monitoring, achieving submillimeter accuracy with maximum deformation of 4.96 mm and a natural frequency of 0.20 Hz.

- Erlandson et al. (2010) developed photogrammetric methods for detecting measurement errors and analyzing point-specific geometrical variations.

2. Recent Technological Developments:
- Zhang et al. (2023) highlighted GNSS-based monitoring methods for real-time structural safety assessment.
- Wang et al. (2023) explored AI and machine learning integration for automated deformation detection and predictive maintenance.

3. Comparative and Technological Assessments:
- Chen and Li (2022) compared monitoring technologies (GNSS, InSAR, drone-based systems), evaluating their accuracy, cost-effectiveness, and scalability.
- Rodriguez et al. (2023) emphasized monitoring strategies in seismically active regions.
- Kim et al. (2023) investigated affordable monitoring solutions for developing regions.

4. Future Research Directions:
- Li and Wang (2023) identified emerging trends, including satellite-based remote sensing and advanced data analytics, calling for interdisciplinary collaboration to advance monitoring practices.

The research underscores the importance of sophisticated deformation monitoring techniques in understanding and mitigating structural health risks.

II. Materials And Method

Study Area

Located in the heart of the developed campus area, facing the sports complex, the Afe Babalola Hall stands as the primary administrative center of the Federal Polytechnic, Ado-Ekiti, in Ekiti State, Nigeria. This three-story administrative building was officially inaugurated on September 27, 2001, and houses a total of 103 offices. It serves as the central hub for key administrative personnel, including the Rector, Deputy Rector (Academics), Registrar, and other important administrative officers. As a significant architectural landmark of the institution, the hall plays a crucial role in the management and operations of this prominent higher education institution in Ado-Ekiti, the capital city of Ekiti State.

(a) Front view **(b) Back view**

Figure 1: Afe Babalola Administrative Building the Federal Polytechnic Ado-Ekiti

Data

In this research work, both primary and secondary data were used. The primary data are the coordinates of demarcated points obtained from the field. These include the northing, easting and heights of all the demarcated points. The secondary data are the information derived from journals, reviews, magazines, newspaper and other online resources. Also used are the coordinates, obtained from the Survey Department of the institution, of the existing survey points which were used as controls for referencing the new points.

Methodology

For the preliminary stages of observation, six control points were carefully examined and verified. Specifically, three control points (FPA164S, FPA165S, and FPA09S) were designated for marking the front view, while the remaining three points (FPA06S, FPA05S, and FPA07S) were assigned to delineate the back view of the structure. Upon thorough inspection, all control points were confirmed to be situated in their precise intended locations, with their corresponding coordinates systematically documented in the accompanying table.

Table 1: Coordinates of control Points

Beacon Names	NORTHINGS(m)	EASTINGS(m)	HEIGHT(m)
FPA164S	840006.130	753778.958	377.003
FPA165S	840088.879	753511.911	367.858
FPA09S	839720.839	753733.436	371.689
FPA06S	839900.292	753469.419	378.300
FPA05S	839929.394	753330.634	376.011
FPA07S	839863.574	753637.776	368.615

The building's demarcation involved six strategic points: three points at the front labeled QA, QB, and QC, and three points at the back labeled PA, PB, and PC. The sides of the building remained unmarked due to structural limitations. Concrete nails were utilized for point placement, with black-colored paint creating circular markers to enhance point visibility and recognition.

Coordinate determination was accomplished using a total station instrument, with each point meticulously observed six times at monthly intervals. The observation period commenced on May 10th and concluded on October 10th, 2024, spanning a comprehensive six-month monitoring timeframe.

For deformation monitoring, the research employed the Root Mean Square (RMS) statistical technique. As described by Jones (2018), RMS is a mathematical method that calculates the square root of the average squared differences between individual data points and their mean. This approach serves multiple analytical purposes, including measuring data magnitude, calculating population standard deviation, and evaluating data point deviations from the mean.

The RMS method provides a robust statistical approach to quantifying and analyzing structural variations by systematically assessing the variations and dispersions within the collected dataset.

RMS= $\sqrt{(\Sigma(x_i - \mu)2/N)}$…………………………(1)

Where:

X_i= individual data points

μ= mean of the data points

N= number of data points

Σ= summation symbol.

The research utilized Microsoft Excel to perform statistical analysis, examining the correlations among the dataset, deformation mode, and deformation direction. Using AutoCAD 2010, a comprehensive deformation plan was created by plotting the three-dimensional coordinates (X, Y, and Z) of selected observation points, tracking their horizontal and vertical movements over a six-month period.

III. Results

This section presents the comprehensive findings derived from field observations, featuring a detailed tabulation of the coordinates for the previously demarcated points. The table provides a systematic representation of the spatial data collected during the monitoring process, offering a clear and structured overview of the point-specific coordinate measurements obtained through meticulous field research.

Table 2: Coordinates of Demarcated Points

DATE	POINT	Northing	Easting	Heights
09/05/2024	QA	839966.072	753567.239	368.105
	QB	839962.146	753580.005	368.107
	QC	839950.494	753620.294	367.850
	PA	839868.067	753630.979	378.770
	PB	839868.794	753613.994	381.256
	PC	839864.794	753632.217	384.178
10/06/2024	QA	839966.060	753567.242	367.304
	QB	839962.776	753580.071	367.324
	QC	839950.571	753620.287	367.251
	PA	839865.146	753630.865	378.075
	PB	839868.642	753613.720	381.661
	PC	839864.600	753632.437	384.200
10/07/2024	QA	839966.106	753567.193	367.320
	QB	839962.762	753580.053	367.323
	QC	839950.496	753620.269	367.244
	PA	839865.127	753630.900	378.252
	PB	839868.817	753613.800	381.376
	PC	839864.612	753632.500	384.018
10/08/2024	QA	839966.094	753567.159	367.096

	QB	839962.797	753580.096	367.089
	QC	839950.494	753620.284	367.555
	PA	839865.132	753630.815	378.352
	PB	839868.714	753613.839	381.400
	PC	839864.542	753632.488	384.011
09/09/2024	QA	839966.122	753567.197	367.200
	QB	839962.717	753580.072	367.201
	QC	839950.513	753620.351	367.134
	PA	839865.250	753630.915	378.254
	PB	839868.825	753613.884	381.414
	PC	839864.558	753632.414	384.025
	QA	839966.101	753567.243	367.121
10/10/2024	QB	839962.774	753580.069	367.101
	QC	839950.533	753620.294	367.198
	PA	839865.27	753630.814	378.23
	PB	839868.9	753613.645	381.4
	PC	839864.4	753632.358	384.027

Mean of northing, easting, height, their deviations and root mean square was done using the Ms Excel spreadsheet. The results are shown in Table 3 to Table 9 in this section.

Table 3: Mean (µ) of Northing and Deviations

Mean µ	Point 1	Point 2	Point 3	Point 4	Point 5	Point 6
	839966.093	839962.662	839950.517	839865.165	839868.782	839864.584
$X_1 - \mu$	-0.021	-0.516	-0.023	-0.098	0.012	0.21
$X_2 - \mu$	-0.033	0.114	0.051	-0.019	-0.140	0.016
$X_3 - \mu$	0.013	0.100	-0.021	-0.038	-0.170	0.028
$X_4 - \mu$	0.001	0.135	-0.023	-0.033	-0.068	-0.042
$X_5 - \mu$	0.029	0.055	-0.004	0.085	0.043	-0.026
$X_6 - \mu$	0.008	0.112	0.016	0.105	0.118	-0.184
Σ	-0.003	0	-0.001	0.002	-0.205	0.002

Table 4: Mean (µ) of Easting and Deviations

Mean µ	Point 1	Point 2	Point 3	Point 4	Point 5	Point 6
	753567.212	753580.061	753620.297	753630.881	753613.814	753632.402
$X_1 - \mu$	0.027	-0.056	-0.003	0.098	0.18	0.185
$X_2 - \mu$	0.03	0.01	-0.01	-0.016	-0.094	0.035
$X_3 - \mu$	-0.019	-0.008	-0.028	0.019	-0.014	0.098
$X_4 - \mu$	-0.053	0.035	-0.013	-0.066	0.025	0.086
$X_5 - \mu$	-0.015	0.011	0.054	0.034	0.07	0.012
$X_6 - \mu$	0.031	0.008	-0.003	-0.067	-0.169	-0.044
Σ	0.001	0	-0.003	0.002	-0.002	0.372

Table 5: Mean (µ) of Height and Deviations

Mean µ	Point 1	Point 2	Point 3	Point 4	Point 5	Point 6
	367.358	367.358	367.372	101.322	102.251	102.153
$X_1 - \mu$	0.747	0.751	0.478	0.448	0.005	0.025
$X_2 - \mu$	-0.054	-0.032	-0.121	0.247	0.41	0.047
$X_3 - \mu$	-0.038	-0.033	-0.128	-0.07	0.125	-0.135
$X_4 - \mu$	-0.262	-0.2670	0.183	0.03	0.149	-0.142
$X_5 - \mu$	-0.158	-0.164	-0.171	-0.068	0.163	-0.128
$X_6 - \mu$	-0.237	-0.255	-0.174	-0.092	0.149	-0.126
Σ	0.2338	0	0.067	0.495	1.001	-0.3438

Table 6: Root Mean Square of Northing

Data Point	Point 1	Point 2	Point 3	Point 4	Point 5	Point 6
	$(X_i - \mu)^2$	$(X_i - \mu)^2$	$(X_i - \mu)^2$	$(X_i - \mu)^2$	$(X_i - \mu)^2$	$(X_i - \mu)^2$
X_1	0.000441	0.266256	0.000529	0.009604	0.000144	0.0441
X_2	0.001089	0.012996	0.002916	0.000361	0.0196	0.000256
X_3	0.000169	0.01	0.000441	0.001444	0.0289	0.30784
X_4	0.000001	0.018225	0.000529	0.001089	0.004624	0.001764
X_5	0.000841	0.003025	0.0016	0.007225	0.001849	0.000676
X_6	0.0000064	0.012544	0.000256	0.011025	0.013924	0.033856
Σ	0.0025474	0.323046	0.006271	0.030748	0.069041	0.81436
RMS	0.00042	0.053841	0.00105	0.00512	0.01151	0.01357

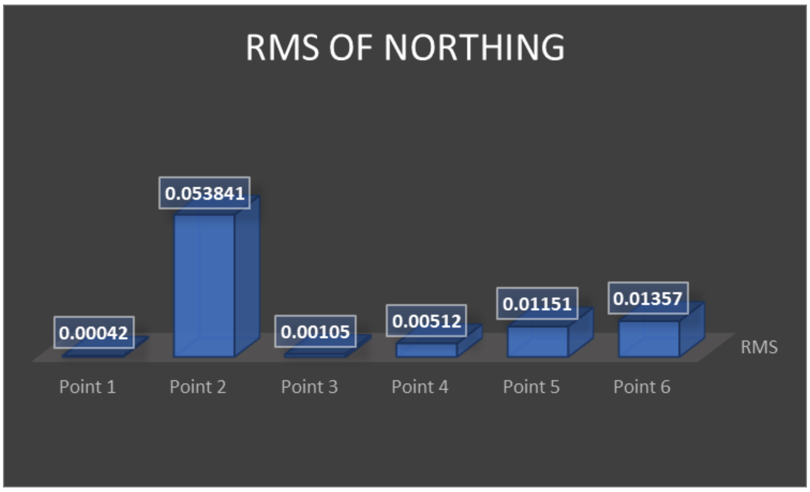

Figure 2: Show the RMS of Northing

Table 7: Root Mean Square of Easting

Data Point	Point 1	Point 2	Point 3	Point 4	Point 5	Point 6
	$(X_i - \mu)^2$	$(X_i - \mu)^2$	$(X_i - \mu)^2$	$(X_i - \mu)^2$	$(X_i - \mu)^2$	$(X_i - \mu)^2$
X_1	0.000729	0.003136	0.509	0.009604	0.0324	0.034225
X_2	0.0009	0.0001	0.0001	0.000256	0.008836	0.001225
X_3	0.000361	0.00064	0.000784	0.000361	0.000196	0.009604
X_4	0.002809	0.001225	0.000169	0.004356	0.000625	0.007396
X_5	0.000225	0.000121	0.002916	0.001156	0.0049	0.00144
X_6	0.000961	0.000064	0.00009	0.004489	0.028561	0.001936
Σ	0.005985	0.005286	0.003987	0.020222	0.075518	0.05453
RMS	0.0009975	0.000881	0.0006645	0.003370	0.0125863	0.009088

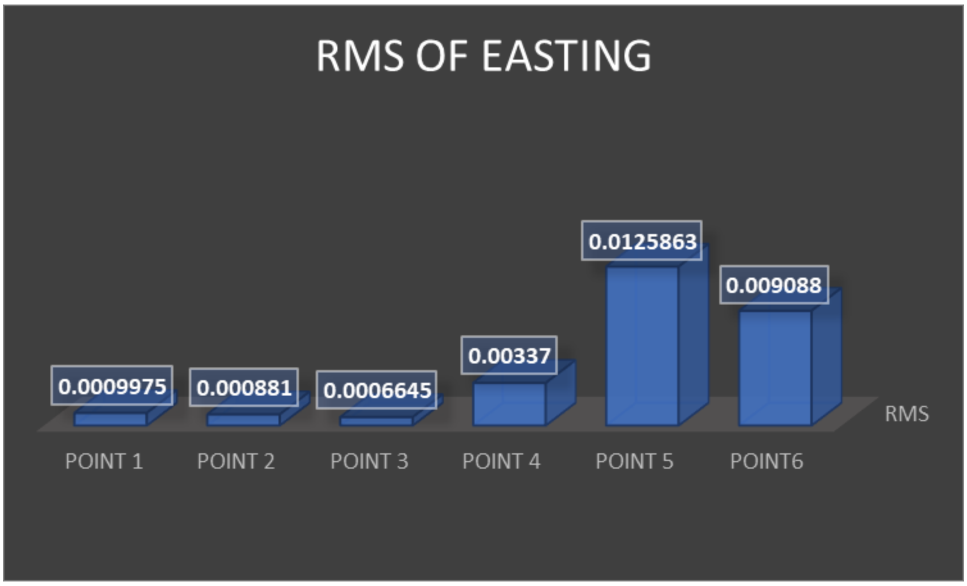

Figure 3: Show the RMS of Easting

Table 8: Root Mean Square of Heights

Data Point	Point 1	Point 2	Point 3	Point 4	Point 5	Point 6
	$(X_i - \mu)^2$	$(X_i - \mu)^2$	$(X_i - \mu)^2$	$(X_i - \mu)^2$	$(X_i - \mu)^2$	$(X_i - \mu)^2$
X_1	0.558009	0.56401	0.228484	0.200704	0.000025	0.000625
X_2	0.002916	0.001024	0.014641	0.061009	0.1681	0.002209
X_3	0.001444	0.001089	0.016384	0.0049	0.015625	0.018225
X_4	0.068644	0.071289	0.033489	0.009	0.022201	0.020164
X_5	0.024964	0.026896	0.029241	0.004624	0.026569	0.016384
X_6	0.056169	0.065025	0.030276	0.008464	0.022201	0.015876
Σ	0.712146	0.729324	0.352515	0.288701	1.767621	0.073483

RMS	0.118691	0.121554	0.0587525	0.0481117	0.294604	0.0122472

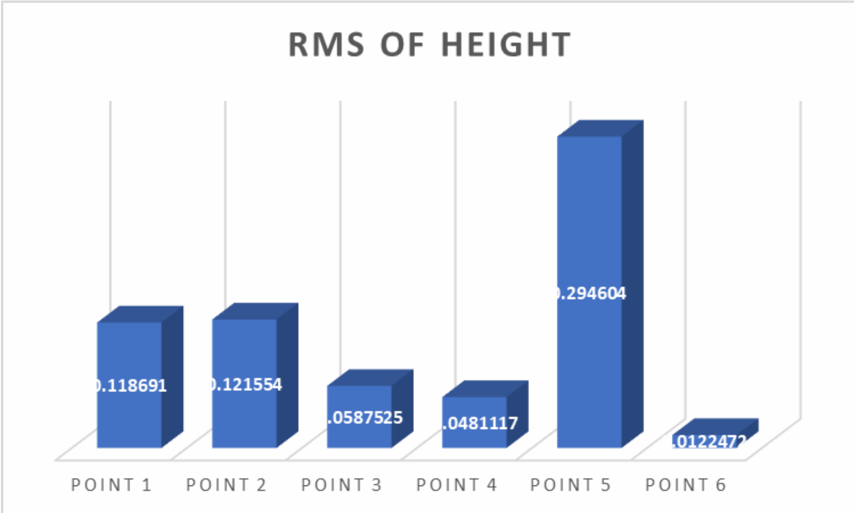

Figure 4: Show the RMS of Height

Table 9: Summary of Root Mean Square (RMS)

Point	Northing	Easting	Height
QA	0.00042	0.0009975	0.118691
QB	0.053841	0.000881	0.121554
QC	0.00105	0.0006645	0.0587525
PA	0.00512	0.003370	0.0481117
PB	0.01151	0.0125863	0.294604
PC	0.01357	0.009088	0.0122472

IV. Discussions

When the RMS is 0 it indicates a perfect match of the data with the initial value. However this is not always the case. A low RMS value tending to zero can be accepted as a good result while an RMS value of 1 and above is not considered as a good result.

From table 9 above the RMS values of point QA for northing, Easting and Heights are 0.00042, 0.0009975 and 0.118691 respectively. This is an indication that the horizontal movement of the building is almost 0 while the vertical movement is a little higher. Similarly, the RMS values of point QC for northing, Easting from same table are 0.00105, 0.0006645 and 0.0587525 respectively. This is an indication that the horizontal movement of the building is almost 0 while the vertical movement is a little higher.

The demarcated points behind the building showed the same pattern of movement. RMS values of point PB for northing, Easting and Heights are 0.01151, 0.0125863 and 0.294604 respectively. This is an indication that the horizontal movement of the building is almost 0 while the vertical movement is a little higher.

The research endeavour to check the correlation between the variables used to ascertain whether the results obtained are reliable or not. The result of the correlation analysis showed that correlation exists amongst these variables i.e. northing, easting and height.

Table 10: Correlation matrix

		northing	easting	height
Correlation	northing	1.000	-.796	-.972
	easting	-.796	1.000	.710
	height	-.972	.710	1.000

Table 11: Test of Significance

Kaiser-Meyer-Olkin Measure of Sampling Adequacy.		.578
Bartlett's Test of Sphericity	Approx. Chi-Square	13.066
	df	3
	Significance	.004

From table 10, there is strong but negative correlation between the northing and both the easting and height, whereas there is strong but positive correlation between the easting and height. Table 11 showed significance value of 0.004 which is lesser than 0.005 significance level meaning that the relationship among the variables if significant.

V. Conclusions

The comprehensive deformation monitoring of the Afe Babalola Building at the Federal Polytechnic, Ado-Ekiti has been completed, providing crucial insights for future structural stability assessments. The study successfully achieved its primary objectives, revealing a consistent pattern of building movement across northing, easting, and height dimensions.

Notably, the analysis demonstrated that horizontal movements (northing and easting) were comparatively minimal, while vertical displacement exhibited more pronounced variations. The research further concluded that a statistically significant and strong correlation exists among the observed variables, suggesting interconnected structural dynamics that warrant careful consideration for long-term building maintenance and potential intervention strategies.

References

[1] Agresti, A., & Finlay, B. (2018). Statistical Methods For The Social Sciences (5th Ed.). Pearson.

[2] Brockwell, P. J., & Davis, R. A. (2016). Introduction To Time Series And Forecasting (3rd Ed.). Springer

[3] Brown, G. G. (2007). Survey Methodology (2nd Ed.). John Wiley & Sons.

[4] Chen, Et Al. (2023). Integration Of Unmanned Aerial Vehicles And Lidar Scanning In Structural Deformation Monitoring: A Review. Journal Of Surveying Engineering. 50(2), 189-204.

[5] Chen, H., & Li, Z. (2022). Comparative Analysis Of Structural Deformation Monitoring Technologies: A Review. Journal Of Structural Engineering, 48(3), 321-335.

[6] Chen, H., Wang, X., & Li, Z. (2018). Applications Of Synthetic Aperture Radar Interferometry (Insar) In Structural Health Monitoring: A Review. Remote Sensing, 10(10), 1608

[7] Chen, H., & Wang, X. (2019). Historical Structure Deformation Analysis Using Advanced Monitoring Techniques: A Case Study. Journal Of Cultural Heritage, 36, 123-130.

[8] Erlandson, J. C. Peterson, And Veress S. A. (2010). Performance Observations Formations By Photogrammetric Methods, Technical Reports Part I And II. U. S. Corps Of Engineers, Seattle District

[9] ESRI. (2012) Arcgis Desktop: Release 10.9, Environmental Systems Research Institute, Redlands, California, United States.

[10] Frändin, M., &Gabestad, H. (Eds.). (2011). Transport And Accessibility At Home And Abroad: Comparing The Results Of Eurostat's Survey On EU Transport And Accessibility. Edward Elgar Publishing.

[11] Gupta, A., & Patel, R. (2022). Integrating Drone Technology With Surveying Methods For Structural Deformation Monitoring. Journal Of Construction Engineering And Management, 148(1), 04021029.

[12] Garcia-Hernandez, A., Pozuelo, M., & Carrion, J. (2016). Integration Of Continuous Structural Health Monitoring In A Large Infrastructure Project: A Case Study. Structure And Infrastructure Engineering. 12(2), 213-227.

[13] Johnson, E., & Williams, S. (2018). Seismic Activity And Structural Deformation: A Case Study Of The San Andreas Fault. Earthquake Engineering And Structural Dynamics, 47(5), 1119-1136.

[14] Jones, Alan R. (2018). Probability, Statistics And Other Frightening Stuff L. Routledge. P. 48.ISBN 9781351661386. Retrieved 5 July 2020.

[15] Kim, S., (2023). Structural Deformation Monitoring In Developing Regions: Challenges And Opportunities. Journal Of Civil Engineering, 15(2), 187-201.

[16] Li, J., & Chen, W. (2019). Impact Of Subsidence On Bridge Structures: A Case Study. Journal Of Geotechnical And Geoenvironmental Engineering, 145(8), 04019037.

[17] Li, J., Liu, W., & Wang, Y. (2020). Dam Deformation Monitoring: A Case Study Using GNSS And Traditional Surveying. Journal Of Water Resources Planning And Management, 146(9), 04020073.

[18] Li, X., Zhang, Q., & Wang, Y. (2022). Satellite-Based Remote Sensing Technologies For Infrastructure Deformation Monitoring: A Comprehensive Review.Sensors, 22(2), 575.

[19] Li, X., Liu, J., & Zhang, Q. (2021) Advances In GNSS-Based Structural Deformation Monitoring. Sensors, 21(15), 5097.

[20] Moore J.F.A. (1992). Monitoring Building Structures. Blackie And Son Ltd. ISBN 0-216- 93141-X, USA And Canada ISBN 0-442-31333-0

[21] Rodriguez-Castro, R., & Perez-Garcia, J., (2018). Environmental Factors Influencing Structural Deformation: A Case Study. Engineering Failure Analysis, 94, 217-226.

[22] Rodriguez, R., (2023). Regional Perspectives On Structural Deformation Monitoring: Case Studies From Seimically Active Regions. Journal Of Earthquake Engineering, 10(4), 512-526.

[23] Schuurmans, W. (Ed.). (2004). Environmental Modelling: An Introduction (2nd Ed.). Oxford University Press.

[24] Smith, M. P., & Crooks, A. T. (Eds.). (2011). Complexity Theories Of Cities Have Come Of Age: An Overview With Implications To Urban Planning And Design. Springer.

[25] Smith, P., & Johnson, E. (2023). Meta-Analysis Of Structural Deformation Monitoring Data: Patterns And Trends. Journal Of Structural Health Monitoring, 22(1), 78-92.

[26] Smith, P., Brown, A., & Davis, M. (2020). Continuous Structural Deformation Monitoring For Preventive Maintenance: A Case Study. Structural Health Monitoring, 19(3), 617-634.

[27] Wang, J., Et Al. (2023). Integration Of Artificial Intelligence And Machine Learning In Structural Health Monitoring: A Systematic Review. Automation In Construction, 47, 123-137

[28] Wang, Y., Chen, Q., & Zou, Q. (2017). High-Rise Building Deformation Monitoring Using Insar Technology. ISPRS International Journal Of Geo-Information, 6(11), 359.

[29] Wang, J., & Li, H. (2019). Predictive Capabilities Of Structural Health Monitoring: A Case Study. Journal Of Performance Of Constructed Facilities, 33(4), 04019046.

[30] Zhang, Et Al. (2023). Review Of GNSS-Based Structural Deformation Monitoring Methods: Current Status And Future Prospects. Sensors, 23(2), 145-158.

[31] Zienkiewicz, O. C., Taylor, R. L, & Zhu, J. 2. (2005). The Finite Element Method: Its Basis And Fundamentals (6th Ed.). Butterworth-Heinemann.